RANBP1 localizes a subset of mitotic regulatory factors on spindle microtubules and regulates chromosome segregation in human cells

Antonio Tedeschi*, Marilena Ciciarello, Rosamaria Mangiacasale, Emanuele Roscioli, Wilhelmina M. Rensen and Patrizia Lavia‡

IBPM Institute of Molecular Biology and Pathology, CNR National Research Council, Via degli Apuli 4, 00185 Rome, Italy

*Present address: Research Institute of Molecular Pathology (IMP), Dr Bohr-Gasse 7, A-1030 Vienna, Austria

‡Author for correspondence (e-mail: patrizia.lavia@uniroma1.it)

Accepted 28 August 2007
Journal of Cell Science 120, 3748-3761 Published by The Company of Biologists 2007
doi:10.1242/jcs.009308

Summary

The GTPase RAN has an established role in spindle assembly and in mitotic progression, although not all mechanisms are fully understood in somatic cells. Here, we have downregulated RAN-binding protein 1 (RANBP1), a RAN partner that has highest abundance in G2 and mitosis, in human cells. RANBP1-depleted cells underwent prolonged prometaphase delay often followed by apoptosis. Cells that remained viable assembled morphologically normal spindles; these spindles, however, were hyperstable and failed to recruit cyclin B1 or to restrict the localization of HURP (DLG7), a microtubule-stabilizing factor, to plus-ends. RANBP1 depletion did not increase the frequency of unattached chromosomes; however, RANBP1-depleted cells frequently showed lagging chromosomes in anaphase, suggesting that merotelic attachments form and are not efficiently resolved. These data indicate that RANBP1 activity is required for the proper localization of specific factors that regulate microtubule function; loss of this activity contributes to the generation of aneuploidy in a microtubule-dependent manner.

Supplementary material available online at
http://jcs.biologists.org/cgi/content/full/120/21/3748/DC1

Key words: RANBP1, GTPase RAN, Mitosis, Spindle microtubules, HURP, Cyclin B1

Introduction

The GTPase RAN is a well-known regulator of nucleo-cytoplasmic transport across the nuclear envelope (NE) in interphase, of spindle organization after NE breakdown, and of nuclear and NE reconstitution at mitotic exit (reviewed by Weis, 2003). Although diverse, these functions rely on one basic conserved mechanism: the ability of GTP-bound RAN to interact with its effectors. RAN effectors essentially belong to the family of transport vectors [e.g. importin β and exportin (CRM1, XPO1)] and after NE breakdown are functionally 'recycled' from their role as transport vectors to act as mitotic regulators.

The nucleotide-bound state of RAN is regulated by the nucleotide exchange factor RCC1, which generates GTP-bound RAN (RAN-GTP), and by RANGAP1, which catalyzes GTP hydrolysis on RAN. RAN-binding protein 1 (RANBP1) is a non-catalytic partner that regulates nucleotide turnover on RAN by modulating the activity of RAN catalytic factors: it stimulates hydrolysis by RANGAP1 and inhibits RCC1 activity, at least in vitro (Bischoff et al., 1995). Physiological roles of RANBP1 are probably more complex, because RANBP1 is found in complexes with RAN and transport factors (Plafker and Macara, 2002), and it contributes to modulate the assembly and disassembly of these complexes (Chi et al., 1996; Kehlenbach et al., 1999).

Mitotic roles of RAN, its regulators and effectors were originally identified in *Xenopus* egg-derived systems, in which spindle assembly is driven by chromatin and requires RAN-GTP. Seminal studies showed that RAN-GTP regulates mitosis essentially by acting on classical import complexes containing mitotic factors that harbour a nuclear localization sequence (NLS), an importin α member interacting with the NLS and importin β, the import vector in interphase (Carazo-Salas et al., 1999; Kalab et al., 1999). RAN-GTP binds importin β with high affinity and causes the release of free NLS factors that can then productively regulate mitotic processes. RAN-GTP is generated by chromatin-bound RCC1 and is hydrolyzed away from chromatin: therefore, free NLS-containing mitotic factors are prevalently released in the proximity of chromatin. This is consistent with the mechanism of chromatin-driven spindle assembly. These data support the idea that a 'gradient' of RAN-GTP that concentrates at chromosomes, and dilutes away from them, regulates spindle formation and function in the *Xenopus* model (Caudron et al., 2005).

Despite the conservation of the basic mechanisms in the RAN network, we do not fully understand how RAN operates to regulate mitosis after spindle assembly in mammalian cells. The gradient model explains long-range effects, but does not seem to explain the diversity and specificity of events that are influenced by RAN, namely aster organization, spindle pole formation and microtubules (MTs)/kinetochores (KTs) interactions (reviewed by Arnaoutov and Dasso, 2005; Ciciarello et al., 2007). Modelling studies actually indicate that the size constraints of somatic cells would limit the

efficacy of the gradient (Gorlich et al., 2003; Kalab et al., 2006). Rather, increasing evidence from somatic cells suggests that local assemblies of RAN regulators and effectors 'embedded' within the overall RAN gradient produce subtle signals at centrosomes, MTs and KTs. These signals can generate local discontinuity in the gradient at crucial mitotic sites. Furthermore, an increasing number of mitotic regulators, including non-NLS factors, are proving responsive to regulation by RAN-GTP (Ciciarello et al., 2007), suggesting that RAN-GTP does not solely operate via disassembly of 'classical' NLS-importin complexes. Together, these lines of evidence indicate that RAN-dependent mechanisms must satisfy more complex and finely tuned layers of control in cells.

Studies in somatic cells have largely relied on overexpression of RAN network components. Although overexpression has been useful to elucidate the localization-function relationship for members of the network, eliminating the activity of specific members should ultimately provide insight into their role during the mitotic division. Thus far, this approach has been limited to RCC1, for which a temperature-sensitive allele exists that can be inactivated in a conditional cell line; the results of inactivation experiments indicate that RCC1 is required for the G2/M transition and in the spindle checkpoint (reviewed by Moore, 2001; Arnaoutov and Dasso, 2005).

RAN network members have been inactivated by RNA interference (RNAi) in *Caenorhabditis elegans*, revealing differential roles of RAN, its regulators and effectors in spindle assembly and NE reformation after mitosis (Askjaer et al., 2002; Bamba et al., 2002). In mammalian cells, RNAi has been employed to inactivate only RANBP2, a SUMO-ligase that regulates the subcellular localization of RANGAP1 but has no direct activity on the RAN cycle: these experiments demonstrated that the RANBP2-RANGAP1 complex regulates the residency of spindle checkpoint factors at KTs (Salina et al., 2003; Joseph et al., 2004). Members of the RAN network 'core' have not been inactivated in somatic cells thus far.

RANBP1 is the only cell cycle-regulated member of the RAN network in mammalian cells, with highest levels from early G2 to anaphase (Guarguaglini et al., 2000), suggesting that modulation of RAN-dependent interactions in mitosis requires increased RANBP1 concentrations compared with earlier cell cycle phases. Indeed, RANBP1 has clear mitotic roles in mammalian cells, because overexpression induces spindle pole fragmentation (Di Fiore et al., 2003) and impairs mitotic exit, whereas injection of a specific antibody to RANBP1 renders mitotic MTs resistant to nocodazole (NOC)-induced depolymerization and yields chromosome mis-segregation (Guarguaglini et al., 2000). Thus, RANBP1 contributes to the regulation of spindle organization and dynamics, and its ratio to RAN is of crucial importance to the regulated processes downstream.

We have now employed RNAi to downregulate RANBP1 in human cells. We show that RANBP1 activity is required to ensure the spatial control of specific factors that regulate mitotic MT function. By doing so, RANBP1 regulates chromosome segregation and its inactivation can contribute to the generation of aneuploidy in an MT-dependent manner.

Results

RANBP1 downregulation increases RAN-GTP levels, induces apoptosis and reduces the mitotic index

To investigate the requirement for RANBP1 activity in human cells, we downregulated RANBP1 protein levels by RNAi. Asynchronously cycling U20S osteosarcoma cells were transfected with *RANBP1*-specific small interfering (si) RNA oligonucleotides and analyzed after increasing lengths of incubation. RANBP1 protein abundance decreased by 70% after 40 hours and by 80% after 64 hours of RNAi, compared with that detected in control cultures, which were either untreated (NT) or treated with control siRNAs, including: GL2, against luciferase (Fig. 1A); 116 siRNA, against the murine *Ranbp1* gene, which is related but not identical to the human sequence; and GFP siRNA (supplementary material Fig. S1). The interference was specific and no variations in either RCC1 (Fig. 1A) or RAN (data not shown) abundance were observed. Similar results were obtained with three different siRNAs targeting different regions of the human *RANBP1* gene (supplementary material Fig. S1).

At the single-cell level, RANBP1 signals were barely or not detectable in interfered cells processed for immuno-fluorescence (IF; Fig. 1B). The reduction in RANBP1 levels was associated with a two- to three-fold increase in the overall RAN-GTP content (Fig. 1B), as revealed by incubating cells with the conformational antibody AR12, which reacts with the extended C-terminal region of RAN in the GTP-bound conformation (Richards et al., 1995). AR12 faithfully depicts variations in RAN-GTP levels induced by manipulating RAN regulators: parallel to the increase measured in RANBP1-depleted cells (Fig. 1B), we observed a decreased reactivity in response to RANBP1 overexpression and to RCC1 inactivation, both of which decrease RAN-GTP abundance (supplementary material Fig. S2). Interestingly, some cytoplasmic AR12 signals were observed in RANBP1-interfered cells (Fig. 1B), indicating that RAN-GTP hydrolysis was inefficient in the absence of RANBP1.

RANBP1 depletion yielded morphological changes in cell shape, with a striking reorganization of MTs in the cytoskeleton and a typically elongated morphology (Fig. 1C). Scoring of cells after DAPI and lamin B1 staining visualized a fraction of cells with highly condensed chromatin, which was sometimes fragmented in 'blobs', and accompanied by the loss of lamin B1 integrity, consistent with typical features of apoptotic cells (Fig. 1F). All *RANBP1*-specific siRNAs, but neither GL2 nor murine-specific 116 siRNA yielded a significant increase in apoptosis over time, as revealed by FACS analysis of hypodiploid cells and reactivity to annexin V (Fig. 1E). Concomitant with this, the mitotic index (MI) declined by 50% between 40 and 64 hours of *RANBP1* interference (i.e. when all cells have completed one or two cell cycles) and decreased further after 72 hours (Fig. 1D); after 86 hours, virtually no mitoses were still present in RANBP1-depleted cultures.

RANBP1 depletion hinders mitotic onset and early progression

The finding that RANBP1 downregulation yields a low MI was intriguing. To investigate it further, we developed a protocol to follow-up RANBP1-depleted cultures while they were undergoing synchronous mitotic entry and progression (Fig.

2A). FACS profiles indicated a substantially similar progression from G1/S in both RANBP1-proficient and -deficient cultures, with only a slightly higher accumulation of RANBP1-depleted cells in the G2+M region compared to controls (Fig. 2B). Cyclin B1 and Aurora-A showed a comparable timing of appearance and accumulation regardless

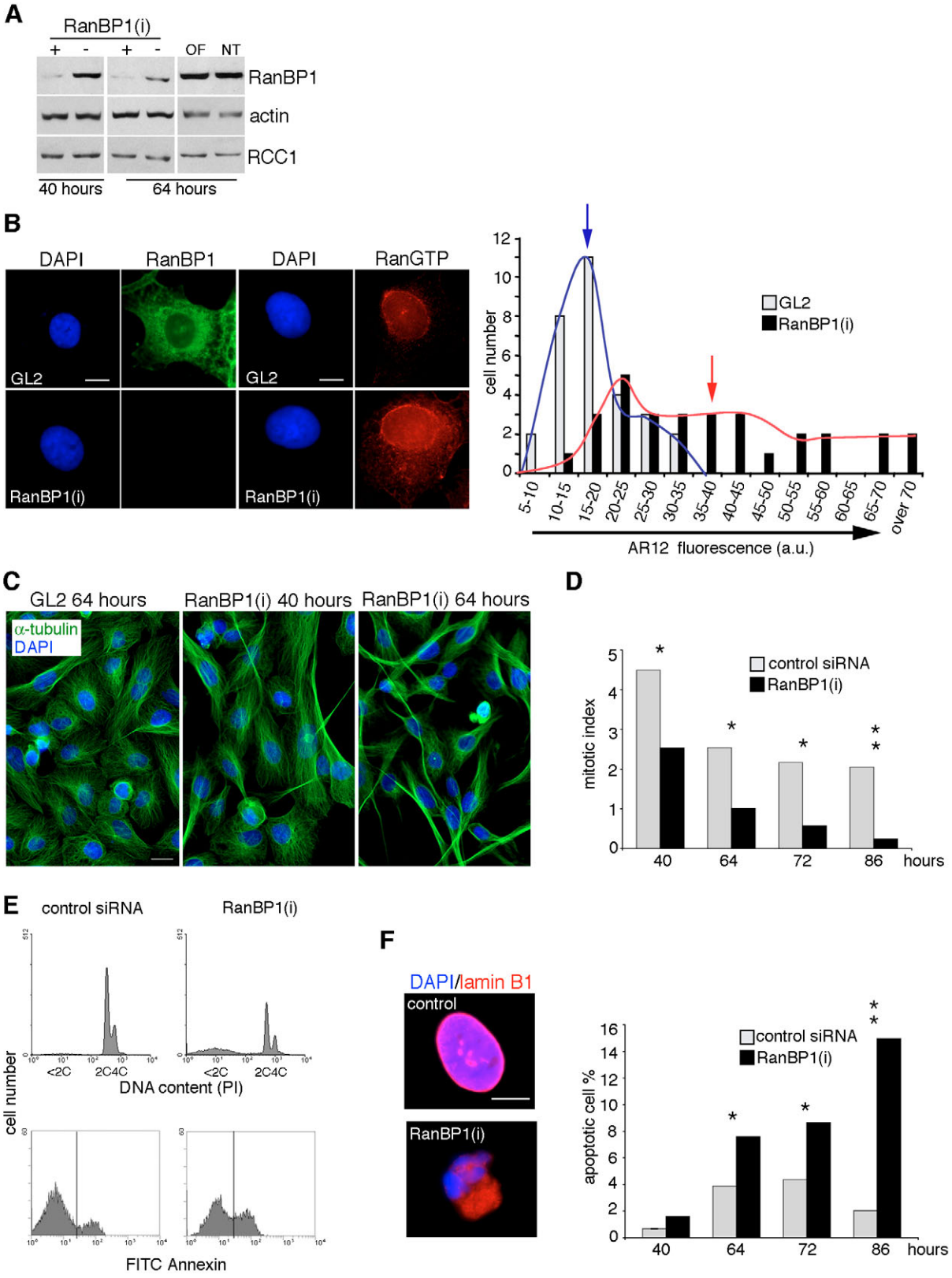

Fig. 1. See next page for legend.

Table 1. In vivo recorded mitotic phenotypes in GL2- and RANBP1-interfered U2OS cells

siRNA	Recorded cells *n*	Early mitotic arrest/ delay* *n*	Early mitotic arrest/ delay* %	Apoptosis *n*	Apoptosis %	Progressing cells *n*	Metaphase duration† mean±s.d.	Abnormal segregation *n*	Abnormal segregation %
GL2	57	2	3.51	0	0.00	55	9.38±4.29	2	3.51
RanBP1-Cy3	80	9	11.25	11	13.75	60	14.31±5.51	10	16.67

*Cells in which the interval from round-up to chromosome alignment lasted >60 minutes were regarded as delayed.
†Metaphase duration was measured from alignment to onset of sister chromatid separation.

of RANBP1 levels (Fig. 2C). However, fewer mitotic figures were scored by microscopy in RANBP1-interfered cells compared to control cultures at all examined times (Fig. 2D); these observations indicate that RANBP1-depleted cells progress with no gross alterations through interphase but are then hindered in M entry and/or early progression. The permanent reduction in the MI observed at all times indicates that RANBP1-depleted cultures do not simply stay longer in G2, with a shifted time of M entry and a delayed mitotic wave, but, rather, a smaller number of cells appear to enter and progress normally through mitosis at all times.

To gain more insight into how low RANBP1 levels might affect mitotic onset and progression, we used *RANBP1*-specific Cy3-tagged siRNA to inactivate *RANBP1* and identify individually interfered U20S cells in synchronized cultures as above, then video-recorded them for 3-4 hours as they reached mitosis. We found that low RANBP1 levels altered mitotic onset and progression at several stages in vivo (Table 1). First, a fraction of RANBP1-interfered cells were delayed, or arrested, in prophase and metaphase: whereas control cells took on average 30 minutes from rounding up to metaphase alignment, RANBP1-depleted cells took an average of 50 minutes; remarkably, some RANBP1-depleted cells remained in a rounded-up stage with condensed chromatin during the entire duration of the video and never reached metaphase (Table 1 and supplementary material Movie 1); another fraction of cells underwent apoptosis after prolonged delay (Table 1 and supplementary material Movie 2). No mitotic cell treated with GL2 siRNA showed any sign of apoptosis, and only a minor fraction were delayed in early mitosis. RANBP1-depleted cells that did not trigger apoptosis and progressed past prometaphase underwent some further delay, but no arrest, in completing metaphase alignment before anaphase onset (Table 1). These data suggest that the spindle checkpoint was transiently activated in RANBP1-depleted cells, possibly associated with impaired MT function; the checkpoint, however, was eventually released and cells progressed to anaphase. Segregation and separation defects eventually became apparent in a fraction of cells (Table 1); chromatin masses often remained trapped in the midzone, and daughter nuclei failed to fully migrate apart.

The localization of RAN-GTP and cyclin B1 at spindle MTs is impaired in RANBP1-interfered cells

The hindrance in early mitotic stages observed in RANBP1-depleted cells suggested that the function of mitotic MTs might be impaired. In previous experiments, a fraction of RAN was seen to colocalize with the spindle MTs in fixed cells (Guarguaglini et al., 2000; Kéryer et al., 2003). It was therefore of interest to determine whether RAN effectors associated with mitotic MTs. In co-sedimentation assays with mitotic MTs, we found that MT pellets contained RAN, importin β and RANBP1 (Fig. 3A), suggesting that dynamic interactions between these components can potentially take place along MTs. The co-sedimentation of RAN was appreciated when MTs were prepared from pure mitotic cells collected by shake-off, but not from cultures released in the cell cycle for many hours after G1/S arrest, in which case MTs represent a mixed population from mitotic and interphase G2 cells: this observation suggests a specific association with mitotic MTs. The association was lost upon MT depolymerization by NOC. This pattern is comparable to that of TPX2, a classical RAN-GTP-dependent MT-associated protein (MAP) (reviewed by Gruss and Vernos, 2004), and HURP, a recently characterized RAN-GTP-regulated factor that binds and stabilizes MTs (Wong and Fang, 2006; Koffa et al., 2006; Silljé et al., 2006).

Fig. 1. RANBP1 downregulation in human U20S cells. (A) Western blotting of the indicated proteins in asynchronously cycling U2OS cultures interfered with *RANBP1*-specific 202 (+) or GL2 (–) siRNA. OF, oligofectamine only; NT, non-transfected cells; RanBP1(i), RANBP1-interfered. (B) Representative RANBP1(i) cells (lower panels) with virtually no RANBP1 signal (green) and elevated RAN-GTP content (red). Bars, 10 μm. The graph (right) shows the distribution of RAN-GTP signal intensity in RANBP1(i) and in GL2-interfered cells. A total of 30 cells per group were randomly selected; the signal was quantified by densitometry and normalized to the cell area; cells were grouped in classes of fluorescence intensity expressed in arbitrary units (a.u.); mean values in the RANBP1(i) (red arrow) and GL2 control (blue arrow) groups are shown. (C) Representative fields from U2OS cultures (40× objective) show morphological changes in cell shape in RANBP1(i) compared with GL2-interfered cultures. Bar, 20 μm. (D) The MI is consistently lower in RANBP1(i) cultures compared with samples incubated with non-specific siRNAs. *P* values indicate statistically significant (*) or highly significant (**) differences between control versus RANBP1(i) cultures using the χ^2 test. (E) FACS analysis of apoptosis in RANBP1(i) and control cultures after 64 hours of RNAi: RANBP1(i) cells accumulate in the <2C region after propidium iodide (PI) staining (upper panels) and show an increased fluorescence intensity after incubation with annexin V (lower panels; viable and apoptotic cells are distributed, respectively, before and after the threshold value of 10 in the logarithmic scale). (F) A representative apoptotic cell from RANBP1(i) cultures (bottom panel); compare to the control cell in the top panel. The graph shows that the percentage of apoptotic cells increases over time in RANBP1(i) cultures and is consistently higher compared with samples incubated with non-specific siRNAs at all time-points studied. *P* values indicate statistically significant (*) or highly significant (**) differences between control versus RANBP1(i) cultures using the χ^2 test. Quantitative results in D and F were obtained from three experiments using two *RANBP1*-specific (202 and 459) and two control (GL2 and 116) siRNAs. A total of 1000-1500 cells were scored for each time-point.

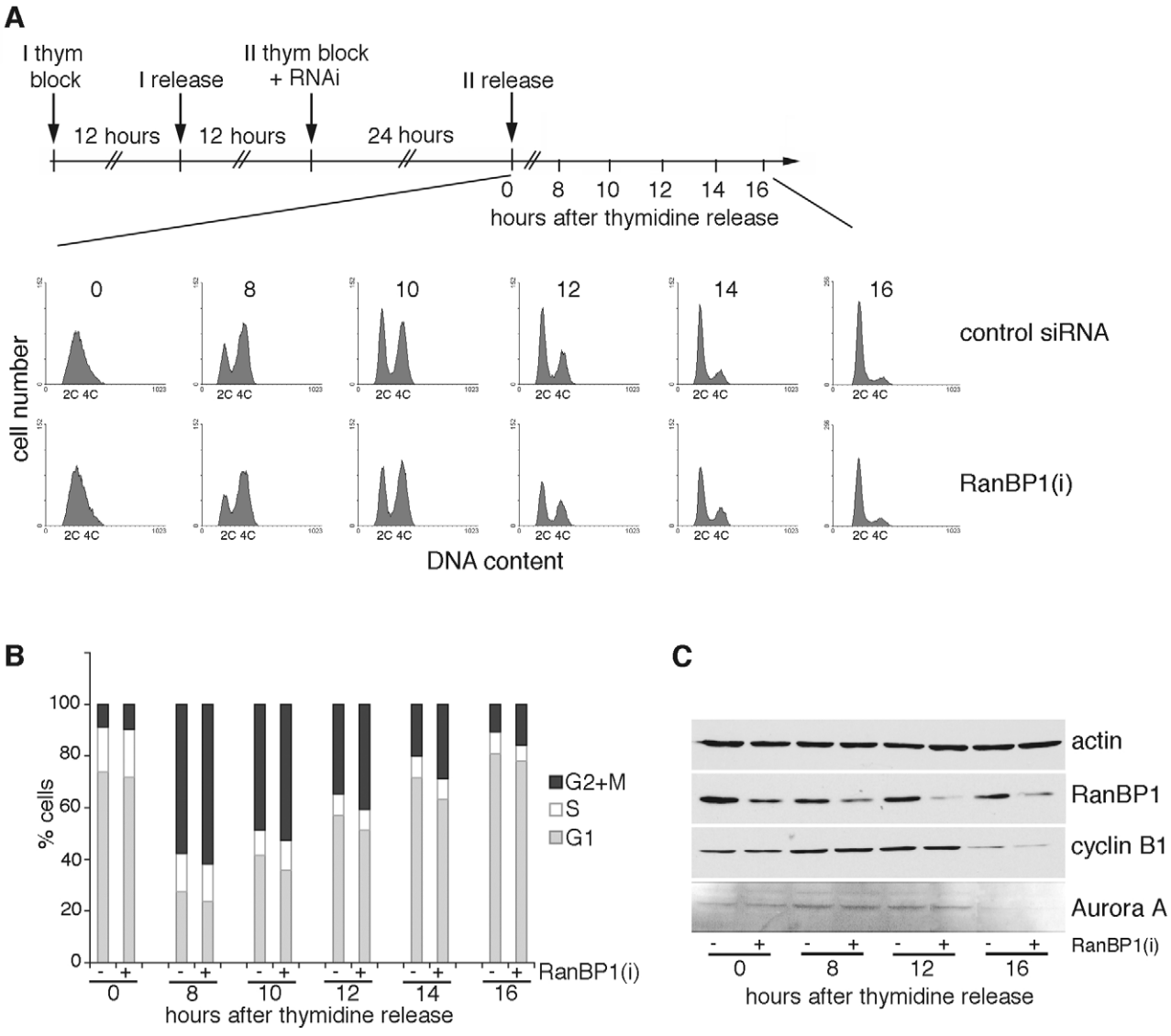

Fig. 2. RANBP1 depletion hinders mitotic entry and progression in synchronously cycling cells. (A) Cell cycle progression in synchronized cultures. Cells were arrested at the G1/S boundary by double thymidine (thym) block, treated with siRNA during the second block, then released to resume cell cycle progression. RANBP1-interfered [RANBP1(i)] and control samples were harvested at regular intervals after thymidine release (time 0) and analyzed by FACS. (B) Histogram representing the proportion of cells in different phases at each time. (C) Western blot analysis of the indicated proteins in RANBP1-interfered (+) and control (–, GL2-interfered) synchronized cultures. (D) Histograms represent the MI scored in RANBP1-interfered and control cultures. *Significant (P<0.01) and **highly significant (P<0.001) differences for each time-point were evaluated using the χ^2 test.

We next investigated whether RANBP1 levels influence RAN-dependent interactions along mitotic MTs. RANBP1 interference did not perturb the establishment of bipolar spindles from asters; in addition, spindles were normal in length, width and total tubulin mass compared to GL2 controls. The distribution of total RAN along the spindle MTs was also comparable in RANBP1- and GL2-interfered mitotic cells (supplementary material Fig. S3). We next used AR12 antibody to investigate whether RANBP1 depletion altered the mitotic distribution of RAN-GTP. When mitotic cells were

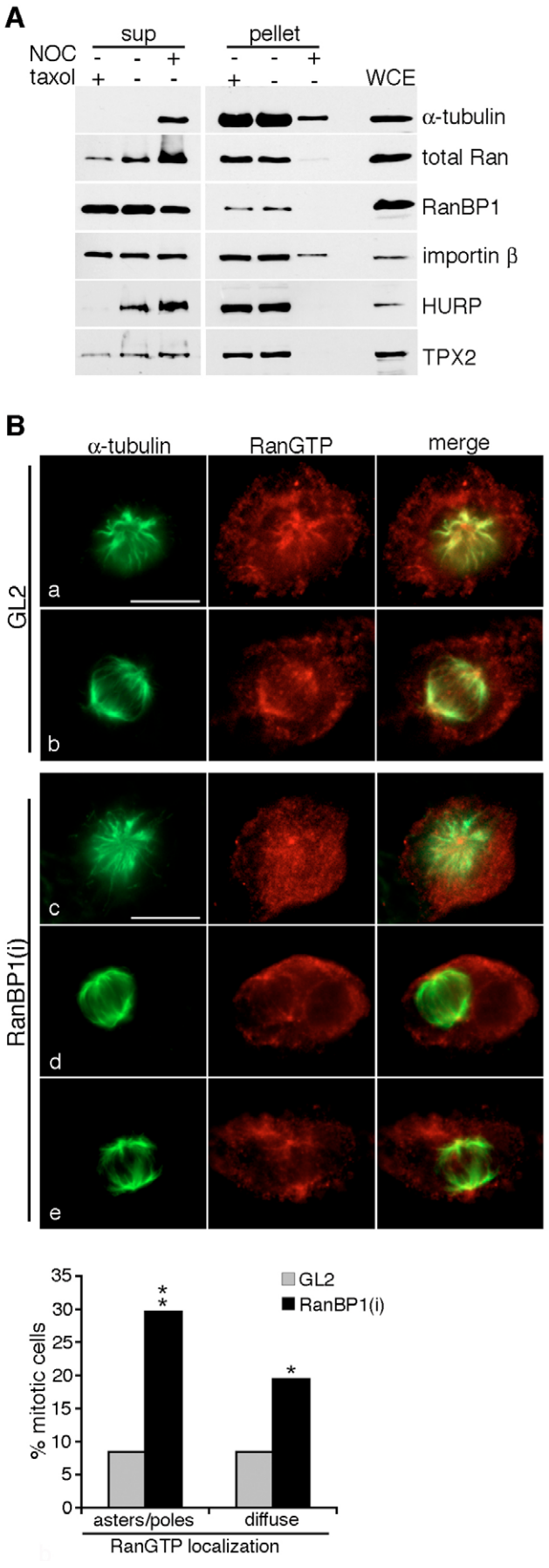

Fig. 3. The mitotic distribution of RAN-GTP is abnormal in RANBP1-interfered mitoses. (A) Co-sedimentation of RAN and its effectors with MTs from mitotic cells treated with buffer (–), NOC or taxol (indicated with +). HURP and TPX2 are shown for comparison. WCE, whole cell extract; sup, supernatant. (B) Localization of AR12-reactive RAN-GTP in control and RANBP1-interfered [RANBP1(i)] prometaphases (a,c) and metaphases (b,d,e). Bars, 10 μm. Graph represents the frequency of RAN-GTP distribution phenotypes in 215 RANBP1- and 210 GL2-interfered cells. The differences were statistically significant (*P<0.02) or highly significant (**P<0.001) using the χ^2 test.

incubated with AR12 prior to fixation, a fraction of RAN-GTP was visualized at asters as well as along the spindle MTs (Fig. 3Ba,b) (see also Kéryer et al., 2003; Ciciarello et al., 2004). This distribution is consistent with that reported in *Drosophila* embryos for RanL43E (a mutant mimicking GTP-bound Ran), which co-localizes with spindle MTs, whereas RanT24N (mimicking GDP-bound Ran) co-localizes with chromatin (Trieselmann and Wilde, 2002). When RANBP1-interfered mitoses were incubated with AR12, localized signals only remained concentrated at asters and spindle poles; AR12 had an otherwise diffuse distribution and failed to colocalize with the spindle MTs (Fig. 3Bc-e). To establish whether RAN-GTP might interact loosely with MTs in RANBP1-depleted cells and might therefore be more easily solubilized than in control cells, we repeated the experiments using extraction protocols of decreasing strength, but still obtained a similar pattern (data not shown). These results indicate that low RANBP1 levels alter the organization of RAN-GTP along the spindle MTs. This was surprising, because the overall RAN-GTP amount increased in RANBP1-interfered cells (Fig. 1). The pattern of total RAN along the spindle MTs was unchanged (supplementary material Fig. S3). Thus, the decreased reactivity to AR12 along MTs suggests that RANBP1 depletion influences interactions that involve RAN-GTP and proteins engaging its C-terminal arm along MTs.

Given that entry and progression in early mitosis were hindered in RANBP1-interfered cells, we next examined cyclin B1 levels. By western blot assays, the timing of onset and accumulation of cyclin B1 were found to be unaltered in RANBP1-interfered cells compared to controls (Fig. 2). In untreated cells, cyclin B1 subcellular localization follows a well-characterized schedule (Hagting et al., 1999; Jackman et al., 2003): it associates with late G2 centrosomes, then enters nuclei at prophase with a fraction remaining at asters, and, after NE breakdown, it associates with MTs and regulates their stability (Verde et al., 1992; Ookata et al., 1995) by directing phosphorylation of specific MAPs. Colocalization experiments with γ-tubulin in synchronized cultures showed that cyclin B1 localization at G2 centrosomes is not affected by RANBP1 interference (data not shown). Furthermore, cyclin B1 entered late G2 and prophase nuclei in a comparable manner in RANBP1- interfered and control cultures (data not shown), consistent with modelling studies that indicate that RANBP1 levels do not substantially affect the rate of nuclear import (Smith et al., 2002; Gorlich et al., 2003). Unexpectedly, however, cyclin B1 failed to associate with MTs in RANBP1-depleted mitoses: Fig. 4A shows RANBP1-interfered cells (identified by Cy3-conjugated siRNA, panels c,d) with cyclin B1 delocalization from asters and spindle MTs; in Fig. 4B,

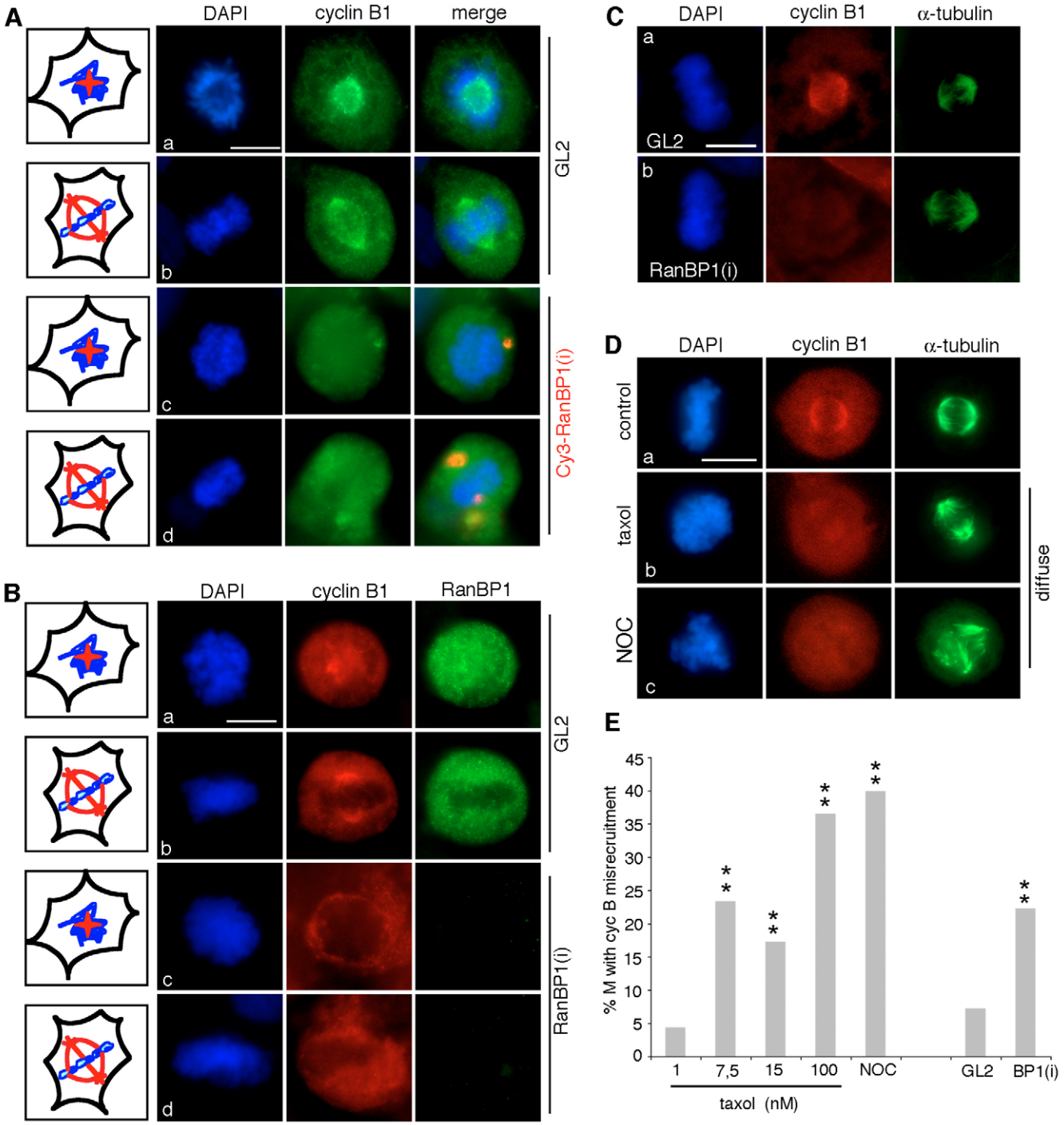

Fig. 4. Impaired association of cyclin B1 with spindle MTs in RANBP1-interfered cells. (A) Cyclin B1 (green) localization in prometaphase (a,c) and metaphase (b,d) cells, identified by DAPI (schematics on the left, in which DNA is blue and MTs red), transfected with GL2 (no colour; a,b) or Cy3-conjugated *RANBP1*-specific siRNA (red; c,d). (B) Cyclin B1 localization in GL2- (a,b) and RANBP1- (c,d) interfered prometaphase (a,c) and metaphase (b,d) cells. RANBP1 depletion can be appreciated in the green channel. (C) Cyclin B1 localization in GL2- (a) and RANBP1- (b) interfered metaphases with morphologically normal spindles, revealed by α-tubulin. (D) Cyclin B1 localization in mitotic cells exposed to taxol (b) or to a dynamics-suppressing NOC dose (c). (a) An untreated metaphase is shown. (E) Frequency of mitotic (M) cells showing cyclin B1 misrecruitment to MTs (200-250 counted mitoses for each condition). **Highly significant differences compared with controls (P<0.001). BP1(i), RANBP1-interfered. Bars, 10 μm.

cyclin B1 delocalization is depicted concomitant with the downregulation of the endogenous RANBP1 protein (panels c,d). The failure of cyclin B1 to localize at MTs was consistently observed even in cells with normal spindle morphology and organization (Fig. 4C).

Cyclin B1 associates poorly with mitotic MTs exposed to

drugs that suppress their dynamics (Bailly et al., 1992). Thus, we compared the pattern of cyclin B1 seen in RANBP1-interfered cells to that of mitotic cells exposed to increasing taxol concentrations, or to a low NOC dose that does not inhibit MT formation but suppresses their dynamics (Ganem et al., 2004). As shown in Fig. 4D, cyclin B1 failed to associate with taxol-stabilized MTs (panel b), or with MTs with impaired dynamics (panel c), in a similar manner to that seen in RANBP1-interfered mitoses (Fig. 4E). Thus, low RANBP1 levels do not affect the localization of cyclin B1 before NE breakdown, but specifically influence its association with mitotic MTs, in a similar manner to that seen in mitotic cells in which MT dynamics is impaired.

RANBP1-depleted cells mislocalize HURP, but not TPX2 or TOGp, on spindle MTs

We wondered whether cyclin B1 mislocalization reflected a generalized failure of mitotic regulators to localize at spindle MTs in RANBP1-depleted mitoses. We therefore decided to examine factors that are directly or indirectly regulated by RAN. We found that RANBP1 interference did not alter the MT localization of TOGp (CKAP5) (Fig. 5A), a MT-stabilizing factor (Charasse et al., 1998; Gergely et al., 2003; Cassimeris and Morabito, 2004) and a component of a RAN-GTP-dependent complex required for spindle formation in the *Xenopus* system (Koffa et al., 2006). TPX2 also associated with MTs, with no obvious difference in its levels or distribution, in RANBP1- and GL2-interfered mitotic cells (Fig. 5B). TPX2 acts in a regulatory loop with the Aurora-A kinase (Tsai et al., 2003) and localizes the latter to MTs (Kufer et al., 2002). We found that Aurora-A also localizes normally to asters and spindle MTs in RANBP1-interfered mitosis (data not shown): thus, neither TPX2 localization, nor its ability to localize Aurora-A, are impaired by RANBP1 depletion.

HURP localizes at MT plus-ends and mediates their attachment to KTs (Wong and Fang, 2006; Koffa et al., 2006; Silljé et al., 2006). In deconvolved images, GL2 cells showed a discrete distribution of HURP, with an almost punctuate appearance, indicative of a spatially restricted concentration at MT plus-ends adjacent to KTs (Fig. 5Ca,b,e,f), as described (Silljé et al., 2006). This localization was altered in RANBP1-depleted mitoses: although the minus-end region of MTs at spindle poles were free of HURP, as in control spindles, HURP had a stretched appearance and distributed over a more extended portion of MTs, rather than concentrating in the plus-end region (Fig. 5Cc,d,g,h). HURP-stained MT regions were also visible across the region occupied by separating chromosomes in anaphase (Fig. 5Cg,h). In synthesis, HURP, but not other MAPs (i.e. TPX2, Aurora-A, TOGp), was specifically affected by RANBP1 depletion for its association with MTs. Thus, RANBP1 depletion influences a subset of RAN-dependent interactions along mitotic MTs.

Mitotic cells with low RANBP1 levels assemble spindles with abnormally stable MTs

In RANBP1-interfered mitoses, both the delocalization of cyclin B1 from spindle MTs, similar to that induced by MT-stabilizing drugs, and the failure to restrict HURP at their plus-ends, were compatible with abnormal functional properties of MTs. We previously found that injecting cells with anti-RANBP1 antibody during mitosis rendered MTs resistant to depolymerization by short pulses of NOC. In order to ascertain whether MTs actually become stabilized in RANBP1-depleted mitotic cells, we assessed their resistance to NOC. Continuous

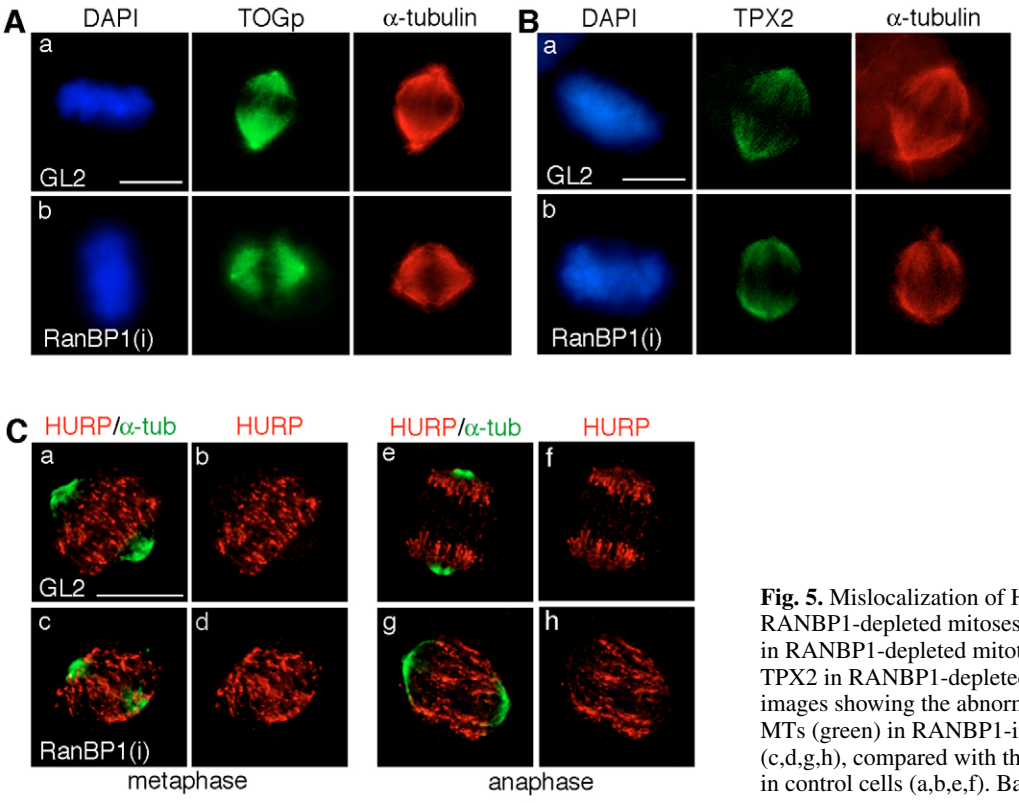

Fig. 5. Mislocalization of HURP, but not TPX2 or TOGp, in RANBP1-depleted mitoses. (A) Unaltered localization of TOGp in RANBP1-depleted mitotic cells. (B) Unaltered localization of TPX2 in RANBP1-depleted mitotic cells. (C) Deconvolution images showing the abnormal organization of HURP (red) over MTs (green) in RANBP1-interfered [RANBP1(i)] mitoses (c,d,g,h), compared with the plus-end-restricted distribution seen in control cells (a,b,e,f). Bars, 10 μm.

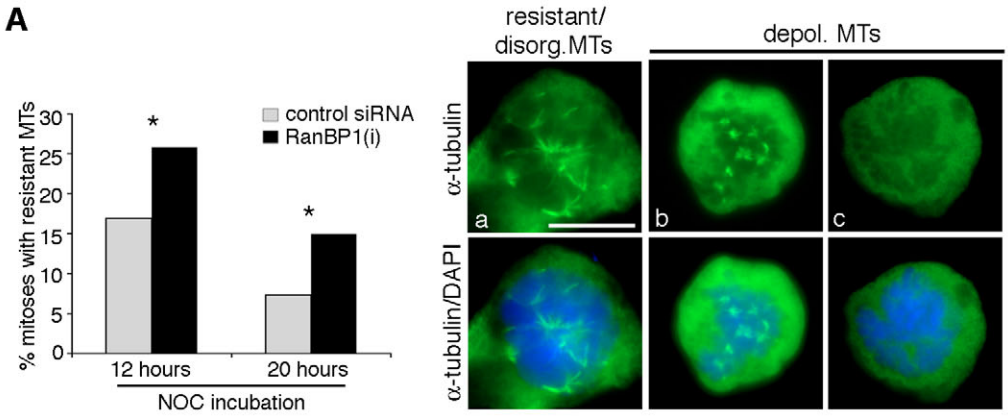

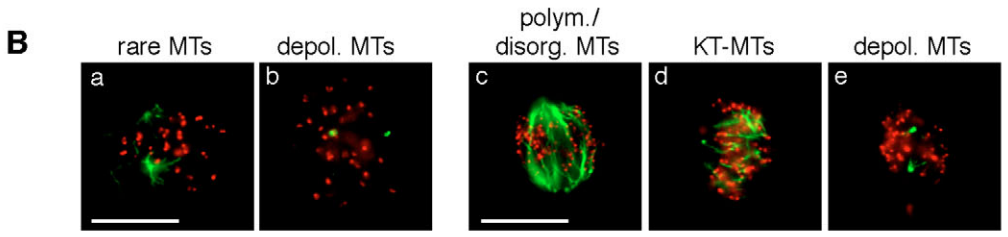

		prophase MTs				prometa / metaphase MTs				
			%				%			
0°C incubation	siRNA	counted mitoses	rare	depol.	p	counted mitoses	polym./ disorg.	KT	depol.	p
10 minutes	GL2	28	35,71	64,29	<0,01	67	31,34	58,21	10,45	<0,05
	RanBP1(i)	22	81,82	18,18		55	54,55	41,82	3,64	
20 minutes	GL2	44	31,82	68,18	<0,05	68	2,94	61,76	35,29	ns
	RanBP1(i)	20	55,00	45,00		30	3,33	70,00	26,67	

Fig. 6. RANBP1-depleted mitoses harbour hyperstable MTs. (A) Graph represents the frequency of mitotic cells with resistant MTs (MTs shown in green in images on right) after 12 or 20 hours of incubation in 50 ng/ml NOC in RANBP1-interfered [RANBP1(i)] cultures and in controls interfered with non-specific siRNAs. Examples of mitotic cells at similar stages that did assemble MTs (indicated as resistant, a) or displaying depolymerized MTs (b,c) are shown on the right. A total of 300 mitotic cells were examined in two independent experiments. *Differences between RANBP1-depleted and controls cells were statistically significant ($P<0.01$) using the χ^2 test. (B) Cold-resistant MTs in GL2- and RANBP1-interfered cells. Representative MT phenotypes are shown (α-tubulin, green; CREST, red); the frequency of each phenotype is quantified in the table below. Statistical differences were calculated using the χ^2 test. ns, non significant. Bars, 10 μm.

NOC treatment (12 or 20 hours) impaired MT assembly in control cells. In RANBP1-silenced cultures, instead, a significant fraction of mitotic cells displayed polymerized MT assemblies, albeit sparse and abnormal in organization (Fig. 6A).

We then analyzed cold-induced depolymerization, which reflects a complementary but distinct phenomenon – the disassembly of MT arrays that had already assembled at the time of incubation – and is regarded as a measure of MT stability. Cells were incubated on ice, then fixed and stained with CREST serum (KTs) and α-tubulin antibody (MTs). In control prophases and prometaphases, three phenotypes of increasing severity were grossly identified (Fig. 6B): cells retaining partly polymerized but somewhat disorganized spindles (panel c); cells displaying residual MT fragments, mostly connected to KTs (panel d); and cells with fully depolymerized MTs, in which tubulin signals only remained at centrosomes (panel e). Among prophases, in which MT stabilization by attached KTs does not yet operate, only two phenotypes were identified: rare residual MT fragments (regarded as cold-resistant, panel a) and fully depolymerized MTs (panel b). RANBP1 depletion yielded a 'protective' effect against depolymerization: when we analyzed prophases and very early prometaphases with unattached chromosomes after 10 minutes on ice, we found that 82% of RANBP1-depleted cells retained resistant MTs, versus 36% in control cells. After 20 minutes, when depolymerization was more extensive, 55% of RANBP1-depleted prophases/early prometaphases still retained resistant MTs or MT fragments. Thus, RANBP1 inactivation results in a strong 'anti-depolymerizing' effect in early mitotic stages. As cells progress to metaphase, MTs attach to KTs and acquire stability. After 10 minutes on ice, residual KT-associated MTs (panel d) became the prevalent phenotype in GL2 metaphases and MTs were only visible in

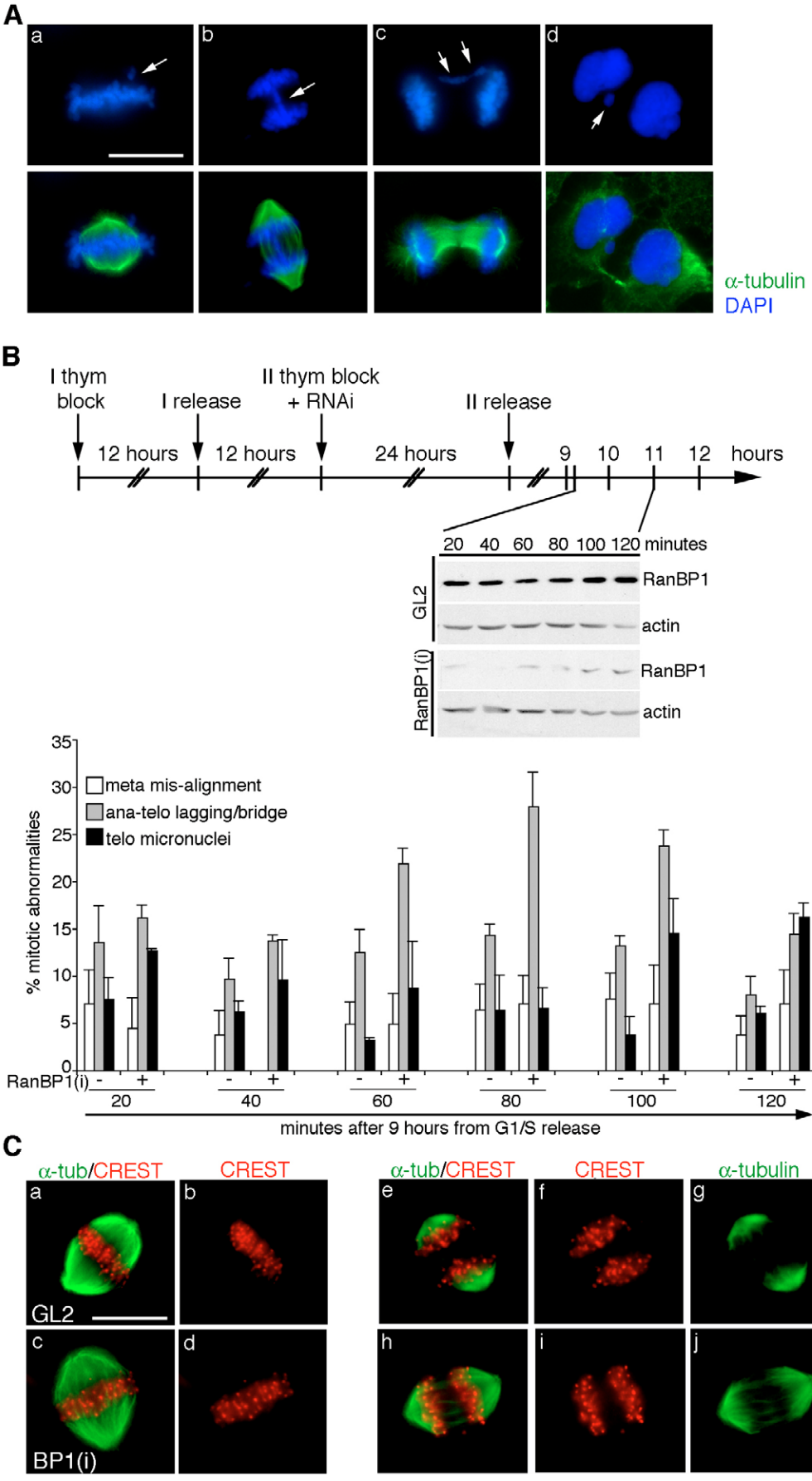

Fig. 7. RANBP1-interfered cells show chromosome segregation defects. (A) Examples of mitotic abnormalities (arrows) in RANBP1-interfered [RANBP1(i)] U20S cells. Bar, 10 μm. (B) Time-course analysis of mitotic abnormalities. The efficiency of RANBP1-interference during synchronization was monitored by western blot. We began to collect mitotic cells 9 hours after release from G1/S arrest; thereafter, samples were harvested every 20 minutes and were examined for mitotic abnormalities. Graph shows the frequency of abnormalities at the indicated times; at least 300 mitotic cells were counted for each time point in two experiments. thym, thymidine; meta, metaphase; ana, anaphase; telo, telophase. (C) Representative metaphase (a-d) showing CREST-stained KTs (red); the left panels show merged pictures with MTs (α-tubulin, green). Anaphase images (e-j) show extending MTs between separating chromosomes in RANBP1- (h-j) but not in GL2- (e-g) interfered cells.

30% of the cells; among RANBP1-interfered metaphases, by contrast, 55% retained largely polymerized, albeit disorganized, MT arrays (Fig. 6Bc). Prolonging the incubation on ice to 20 minutes induced extensive MT depolymerization in both GL2- and RANBP1-interfered cells. Under these more extreme conditions, only KT-associated MTs survived, and their occurrence at this point almost levelled in the RANBP1- and the GL2-interfered late prometaphase and metaphase cells. Thus, RANBP1 depletion increases MT stability particularly before MTs attach to KTs, while exerting a less significant effect after attachment to KTs takes place.

RANBP1-interfered cells display segregation defects during mitotic progression

The observation that MTs are hyperstable in RANBP1-depleted cells prompted us to examine chromosome segregation. To this aim, we decided to analyze mitotic defects in synchronized RANBP1- and GL2-interfered cultures harvested at close intervals to enrich in specific substages during mitotic progression. In metaphase, we occasionally observed incomplete chromosome alignment in RANBP1-depleted cells; in Fig. 7A, one such unaligned chromosome is depicted in panel a, probably reflecting a syntelic attachment. The overall frequency of misalignment, however, was not dramatically different from that scored among GL2 metaphases (Fig. 7B, graph). Furthermore, CREST staining indicated that, by and large, KTs attached completely to MTs (Fig. 7Ca,b). We were therefore surprised to record a significant induction of chromatin bridges and lagging chromosomes that failed to be incorporated into the main set of chromosomes in RANBP1-interfered anaphases (examples in Fig. 7Ab,c); at later times, when cells accumulated in telophase, a significant induction of micronuclei (Fig. 7Ad) became apparent in RANBP1-interfered cultures. The data, summarized in Fig. 7B, indicate that RANBP1 depletion causes a relatively low frequency of chromosome misalignment in metaphase, accompanied by the transient delay revealed in the time-lapse assays (Table 1); eventually, however, RANBP1-depleted cells progress into anaphase; lagging chromosomes become evident at this stage and later evolve in micronuclei that can potentially give rise to aneuploidy. The spindle checkpoint is expected to be functional in RANBP1-interfered cells, because both BUB1 and MAD2 (MAD2L1) are recruited normally to unattached KTs in prometaphase and metaphase, regardless of RANBP1 levels (supplementary material Fig. S4). Furthermore, RANBP1-interfered cells did not bypass the spindle checkpoint in the presence of NOC (supplementary material Fig. S5), indicating that RANBP1 downregulation does not impair the checkpoint response to unattached KTs in cells in which spindle assembly fails.

Merotelic attachments cannot be distinguished in metaphase, but give rise to lagging chromosomes in anaphase. Merotelic attachments form transiently in all cells (Cimini et al., 2003) (reviewed by Cimini and Degrassi, 2005; Musacchio and Salmon, 2007), but in normal conditions they are resolved by a specific pathway requiring Aurora-B and MCAK (Hauf et al., 2003; Kline-Smith et al., 2003; Knowlton et al., 2006). In RANBP1-depleted cultures, the increased frequency of lagging chromosomes and micronuclei in anaphase/telophase, with no detectable abnormalities in metaphase and an intact checkpoint response to NOC, would be compatible with an increased frequency of merotelic attachments. Consistent with that possibility, we noticed that, in RANBP1-depleted cells, MT arrays from opposite poles did often fail to terminate at the most proximal KTs, but seemed to extend past them and across the separating chromosome sets (Fig. 7C, compare panels e-g with h-j). The extended MT configuration did not represent precocious assembly of the central spindle in preparation of cytokinesis, because neither the localization nor the temporal pattern of redistribution of INCENP from KTs to the midzone were influenced by RANBP1 depletion (data not shown). To gain further evidence, we used HeLa cells stably expressing GFP-tagged histone H2B, in which individual chromosomes can be distinguished. We recorded the appearance of lagging chromosomes in 15 out of 47 (32%) RANBP1-interfered mitotic cells in which metaphase alignment was apparently complete (supplementary material Movie 3). This provides direct evidence that lagging chromosomes in RANBP1-depleted cells do not reflect failed chromosome alignment or attachment to MTs. This finding, and the particular features of MTs, suggest, therefore, that RANBP1 depletion yields an increased frequency of merotelic attachments and/or impairs the efficiency of merotelic correction mechanisms.

Discussion

This work represents the first study investigating mitosis after RNAi-mediated downregulation of a RAN network member in mammalian cells. We show that RANBP1 depletion hinders mitotic entry and progression and yields chromosome segregation errors, associated with hyperstability of MTs and mislocalization of cyclin B1 and HURP. Some of these features mirror those previously observed in mitotic cells injected with anti-RANBP1 antibody (Guarguaglini et al., 2000), consistent with the idea that they reflect purely mitotic effects and not secondary consequences to alterations of transport in the previous interphase. Furthermore, the data indicate that particular factors regulating mitotic MT function are selectively impaired when RANBP1 is downregulated, thereby advancing our understanding of the diversified mechanisms of control by RAN in mammalian mitotic cells.

RANBP1 depletion yielded a drastic decrease in the MI, suggesting that M entry is hindered. RANBP1-depleted cells that did enter mitosis took an abnormally long time from round-up (early prophase) to metaphase. The delay in early mitotic stages is at first in contrast with the low MI recorded in RANBP1-depleted cultures. However, the observation that a significant fraction of RANBP1-depleted cells trigger apoptosis during prolonged prometaphase can in fact reconcile this apparent discrepancy and account for both the low MI and the increased apoptosis observed after prolonged RNAi to RANBP1. In a set of independent experiments, we have characterized a specific apoptotic pathway triggered by low RANBP1 levels, which will be reported elsewhere.

RANBP1-depleted mitoses that did not activate apoptosis and progressed through mitosis assembled apparently normal spindles, but MTs were hyperstable, as indicated by their resistance to NOC and to cold-induced MT depolymerization. The latter was particularly evident in early mitotic stages. After attachment to KTs, MTs become stabilized. The ‘protection’ conferred by RANBP1 depletion was less significant after that point, indicating that the status of MTs is sensitive to RANBP1 levels until attachment to KTs takes place.

Related to the finding that MTs are hyperstable in RANBP1-depleted cells, the MT-stabilizing factor HURP was mislocalized over an extended MT portion instead of concentrating at their plus-ends. HURP interacts with importin β directly and dissociates from it when importin β is bound by RAN-GTP (Silljé et al., 2006). In normal cells, this occurs around chromatin, where RAN-GTP is abundant; free HURP then remains concentrated at MT plus-ends (Silljé et al., 2006; Wong and Fang, 2006; Koffa et al., 2006). The extended localization of HURP in RANBP1-depleted cells is reminiscent of that seen in cells transfected with RANQ69L (RAN-GTP-like) mutant (Silljé et al., 2006). RANBP1 is normally enriched at mitotic spindle poles and its concentration decreases towards MT plus-ends, at which HURP normally concentrates. Together, these observations suggest that the correct localization of HURP requires a finely tuned balance between RAN-GTP abundance, for HURP release from importin β, and modulation of RAN activity, which is RANBP1-sensitive, for its restriction at MT plus-ends. These findings might have general implications to understand how RAN complexes are modulated in mammalian cells in vivo.

The earliest identified and best-known RAN-GTP-dependent mitotic factors are regulated via the 'classical' NLS-importin α/β pathway; they form trimeric complexes with importin α and β, and become active when RAN-GTP binds importin β and dissociates the complex. RANBP1 can influence this pathway indirectly by regulating the nucleotide-bound state of RAN. Eliminating RANBP1 facilitates RAN-GTP stabilization: in our experiments, RANBP1 downregulation by 80% increased the intracellular RAN-GTP concentration by around two- or three-fold. We have found that this does not affect the dissociation of classical import complexes such as those containing TPX2: neither TPX2 nor Aurora-A or TOGp were mis-localized in RANBP1-depleted mitoses, nor did TPX2 appear to be any less active than in control mitoses, taking spindle pole integrity (Gruss et al., 2002; Garrett et al., 2002) and Aurora-A localization to MTs (Kufer et al., 2002) as diagnostic features.

A growing number of RAN-GTP mitotic targets, including HURP, are instead being identified as direct importin β partners (reviewed by Ciciarello et al., 2007). The present results strongly suggest that RANBP1 effectively regulates this type of interaction. RANBP1 forms complexes with importin β and RAN (Plafker and Macara, 2002; Nevo et al., 2004); such complexes are thought to represent intermediates in the recycling of transport factors (Chi et al., 1996). RANBP1 can modulate the stability of complexes formed by RAN and its effectors (i.e. importin β itself and CRM1) via direct association and not simply by regulating the nucleotide-bound state of RAN (Plafker and Macara, 2002; Gorlich et al., 2003). In the absence of RANBP1, importin β is expected to bind more stably to RAN-GTP; consequently, cargo factors should be released in a deregulated fashion. Here we show that RANBP1 depletion does indeed yield a decrease of AR12-reactive RAN-GTP (i.e. presumably free from interacting partners along MTs), whereas the association of total RAN with the spindle MTs did not vary. We propose that RANBP1 modulates the dynamic interactions between RAN-GTP and importin β along MTs and, thus, the free or bound state of direct interactors of importin β. The failure to restrict HURP to MT plus-ends would then reflect the formation of unregulated RAN-GTP–importin β complexes along MTs in RANBP1-interfered mitoses. Thus, manipulating RANBP1 levels provides one tool to pinpoint the specificity of control exerted by RAN over factors that are differentially regulated by importin β in mammalian cells.

Mechanistically, the distribution of HURP all over MTs is consistent with their abnormal stabilization and might actually be an underlying cause, given the clear MT-stabilizing activity of HURP in vivo (Wong and Fang, 2006) and in vitro (Santarella et al., 2007). Cyclin B1 also failed to associate with spindle MTs and assumed a diffuse pattern in RANBP1-depleted mitoses; this pattern was similar to that observed in the presence of taxol (Bailly et al., 1992), suggesting that cyclin B1 mislocalization is associated with hyperstabilization of MTs. Interestingly, cyclin B1 phosphorylates HURP (Hsu et al., 2004); it is possible that cyclin B1 mislocalization from MTs affects phosphorylation of HURP and/or other MAPs that regulate MT function.

Chromosome mis-segregation occurs in RANBP1-depleted cells. This mis-segregation does not originate from the failure of MTs to attach to KTs. On the contrary, by and large, MTs attached to KTs and, after transient delay, cells progressed to anaphase. The appearance of segregation errors in anaphase and telophase, with no matching frequency of misaligned chromosomes in metaphase, suggests that merotelic attachments form and are not corrected in RANBP1-depleted cells.

Interestingly, inhibiting CRM1 or RCC1 function also yields segregation errors, as does RANBP1 downregulation, but is associated with a lack of cold-resistant K-fibres (Arnaoutov et al., 2005), a phenotype opposite to that induced by RANBP1 downregulation. Increased levels of RCC1, and hence of chromosomal RAN-GTP, result in override of the spindle checkpoint in the presence of NOC (Arnaoutov and Dasso, 2003). RANBP1 downregulation instead does not impair the checkpoint in response to NOC. It might be speculated that RAN network members and effectors control complementary aspects, with RANBP1 acting to regulate the localization of HURP, and perhaps other importin β-dependent MAPs implicated in MT function, whereas CRM1/RAN-GTP regulate the residency of spindle checkpoint factors at KTs, such that impairing one or the other ultimately impinges on MT-KT interactions in complementary ways.

In conclusion, RANBP1 emerges as an important factor in the correct localization of a subset of proteins that regulate MT function and interaction with KTs: cyclin B1 and HURP are two such factors, probably not the only ones. The finding that RANBP1 downregulation mislocalizes a specific set of factors defines novel aspects of mitotic control by RANBP1. These results begin to shed light on mechanisms through which the RAN network regulates mitotic spindle function in mammalian somatic cells. Further work will be required to elucidate how RAN-dependent complexes are actually regulated along MTs. Pursuing these studies will also be important to understand whether apparently unrelated regulatory systems, such as those operating in MT-KT attachment and correction, are in fact influenced by the RAN pathway.

Materials and Methods

Cell cultures

Cell lines used include human U20S osteosarcoma, HeLa epithelial cells and a HeLa cell line stably expressing H2B-GFP. Where indicated, cell cultures were

synchronized by two rounds of exposure to 2 mM thymidine and release in 30 μM deoxycytidine (both from Sigma Aldrich). In some experiments, cultures synchronized by two rounds of thymidine and released for 7 hours (G2) were exposed to 50 ng/ml or 200 ng/ml NOC for 4 hours; in other experiments, asynchronously cycling and interfered cultures were directly treated with 50 ng/ml or 200 ng/ml NOC for 12 and 20 hours. Cell cycle progression was analyzed by FACS after propidium iodide (PI, Sigma) staining. Apoptotic cells were revealed by PI incorporation or by Annexin-V-FITC (Roche Applied Science) staining. A Coulter Epics XL cytofluorimeter (Beckman Coulter) equipped with EXPO 32 ADC software was used.

RNA interference

Three *RANBP1*-specific siRNA oligonucleotides were synthesized at Qiagen (see sequences in supplementary text and map in supplementary material Fig. S1). Cy3-conjugated 202 siRNA to *RANBP1*, and negative control siRNAs [i.e. GL2, GFP and siRNA 116 (respectively targeting the firefly luciferase, green fluorescent protein and murine RANBP1 coding sequences)], were from Dharmacon Research. siRNAs were used at the final concentration of 60 nM using oligofectamine (Invitrogen).

In vivo recording

Live mitotic cells in Leibovitz's L-15 Medium in 35-mm-diameter dishes were recorded on a 37°C heated stage under an inverted fluorescence microscope (Nikon TE 300) using the ACT-1 software and a DMX1200-type CCD (resolution 1280×1024 pixels). Images were taken every 2 minutes for 3-4 hours (60×/0.7 objective). In some experiments, time-lapse frames were acquired using a 40× EC Plan-Neofluar objective on an Axiovert 200M Cell Observer microscope (Zeiss) controlled by Metamorph software and equipped with a heated XL 295 incubator full-enclosure chamber (Zeiss), MS200 XY Piezo Z Stage (Applied Scientific Instrumentation), and CoolSnapHQ CCD camera. GFP, Cy3 and bright-field frames were recorded every 2 minutes. Time-lapse data were processed using Metamorph and ImageJ (http://rsb.info.nih.gov/ij/) software.

IF and microscopy

Cells grown on sterile coverslips were routinely processed for IF as previously described (Ciciarello et al., 2004). Details of antibodies used and fixation conditions prior to IF are indicated in supplementary material Table S1. Cell preparations were examined under an epifluorescence Olympus AX70 microscope with a CCD camera (Photometrics), or Leica DMR with a CoolSnap (Photometrics). Where indicated, signal intensity and area size were quantified in pixels using Adobe Photoshop on CCD images acquired under identical exposure and gain setting. In deconvolution microscopy, *z*-stack images were taken (0.2 μm distance) using the IAS2000 software (Delta Sistemi) and Autovisualize plus Autodeblur 9.3 deconvolution functions (AutoQuant Imaging).

MT analysis

For MT co-sedimentation assays, MTs were prepared from mitotic HeLa cells collected by shake-off after 10 hours of release from double thymidine block. In vitro polymerization, sedimentation through sucrose and immunoblotting procedures were as described (Ciciarello et al., 2004). To inhibit MT dynamics, cells were treated for 20 hours with concentrations of taxol, ranging from 1 to 100 nM, or with 100 nM NOC (both from Sigma Aldrich). To assess MT resistance to depolymerization, U2OS cells were incubated on ice for 10 or 20 minutes, or cultured in 50 ng/ml NOC, then fixed and processed for IF.

Statistical analysis

All experiments were carried out three times unless otherwise indicated. Samples interfered with *RANBP1*-specific siRNAs (sequences in supplementary material Fig. S1) for the same length of time gave comparable figures for all examined phenotypes, with very low s.d. between independent experiments. Untreated cultures and cultures treated with non-specific siRNAs (GL2 and 116 in most experiments) also gave comparable results with low s.d. The χ^2 test was used to compare figures obtained from pooled observations in control versus RANBP1-interfered cultures. *P* values indicated the statistical significance of the differences between RANBP1- and control-interfered cultures.

We are indebted to Barbara Di Fiore for contributing to early studies in this work. We thank Lynne Cassimeris, Ian Macara, Iain Mattaj, Susanna Nagel, Erich Nigg and Hermann Silljé for reagents. We are grateful to Peter Lenart for help and advice, to Francesca Degrassi, Giulia Guarguaglini and Andrea Musacchio for many insightful discussions, and to Jan-Michael Peters, in whose laboratory some experiments were performed. This work was supported by the Italian Association for Cancer Research (AIRC) and MIUR-FIRB (grants RBIN04T7MT and RBAU01CH2M). M.C. was supported by a FIRC fellowship (Italian Foundation for Cancer Research) and R.M. by a MIUR-FIRB research contract.

Note added in proof

After this work was submitted, a study reporting RNA-interference-mediated inactivation of RANBP1 in mitosis was published (Li et al, 2007).

References

Arnaoutov, A. and Dasso, M. (2003). The Ran GTPase regulates kinetochore function. *Dev. Cell* **5**, 99-111.

Arnaoutov, A. and Dasso, M. (2005). Ran-GTP regulates kinetochore attachment in somatic cells. *Cell Cycle* **4**, 1161-1165.

Arnaoutov, A., Azuma, Y., Ribbeck, K., Joseph, J., Boyarchuk, Y., Karpova, T., McNally, J. and Dasso, M. (2005). Crm1 is a mitotic effector of Ran-GTP in somatic cells. *Nat. Cell Biol.* **7**, 626-632.

Askjaer, P., Galy, V., Hannak, E. and Mattaj, I. W. (2002). Ran GTPase cycle and importins a and b are essential for spindle formation and nuclear envelope assembly in living Caenorhabditis elegans embryos. *Mol. Biol. Cell* **13**, 4355-4370.

Bailly, E., Pines, J., Hunter, T. and Bornens, M. (1992). Cytoplasmic accumulation of cyclin B1 in human cells: association with a detergent-resistant compartment and with the centrosome. *J. Cell Sci.* **101**, 529-545.

Bamba, C., Bobinnec, Y., Fukuda, M. and Nishida, E. (2002). The GTPase Ran regulates chromosome positioning and nuclear envelope assembly in vivo. *Curr. Biol.* **12**, 503-507.

Bischoff, F. R., Krebber, H. R., Smirnova, E., Dong, W. and Ponstingl, H. R. (1995). Co-activation of RanGTPase and inhibition of GTP dissociation by RanGTP binding protein RanBP1. *EMBO J.* **14**, 705-715.

Carazo-Salas, R. E., Guarguaglini, G., Gruss, O. J., Segref, A., Karsenti, E. and Mattaj, I. W. (1999). Generation of GTP-bound Ran by RCC1 is required for chromatin-induced mitotic spindle formation. *Nature* **400**, 178-181.

Cassimeris, L. and Morabito, J. (2004). TOGp, the human homolog of XMAP215/Dis1, is required for centrosome integrity, spindle pole organization, and bipolar spindle assembly. *Mol. Biol. Cell* **15**, 1580-1590.

Caudron, M., Bunt, G., Bastiaens, P. and Karsenti, E. (2005). Spatial coordination of spindle assembly by chromosome-mediated signaling gradients. *Science* **309**, 1373-1376.

Charrasse, S., Schroeder, M., Gauthier-Rouviere, C., Ango, F., Cassimeris, L., Gard, D. L. and Larroque, C. (1998). The TOGp protein is a new human microtubule-associated protein homologous to the Xenopus XMAP215. *J. Cell Sci.* **111**, 1371-1383.

Chi, N. C., Adam, E. J., Visser, G. D. and Adam, S. A. (1996). RanBP1 stabilizes the interaction of Ran with p97 nuclear protein import. *J. Cell Biol.* **135**, 559-569.

Ciciarello, M., Mangiacasale, R., Thibier, C., Guarguaglini, G., Marchetti, E., Di Fiore, B. and Lavia, P. (2004). Importin b is transported to spindle poles during mitosis and regulates Ran-dependent spindle assembly factors in mammalian cells. *J. Cell Sci.* **117**, 6511-6522.

Ciciarello, M., Mangiacasale, R. and Lavia, P. (2007). Spatial control of mitosis by the GTPase Ran. *Cell. Mol. Life Sci.* **64**, 1891-1914.

Cimini, D. and Degrassi, F. (2005). Aneuploidy: a matter of bad connections. *Trends Cell Biol.* **15**, 442-451.

Cimini, D., Moree, B., Canman, J. C. and Salmon, E. D. (2003). Merotelic kinetochore orientation occurs frequently during early mitosis in mammalian tissue cells and error correction is achieved by two different mechanisms. *J. Cell Sci.* **116**, 4213-4225.

Di Fiore, B., Ciciarello, M., Mangiacasale, R., Palena, A., Tassin, A. M., Cundari, E. and Lavia, P. (2003). Mammalian RanBP1 regulates centrosome cohesion during mitosis. *J. Cell Sci.* **116**, 3399-3411.

Ganem, N. J. and Compton, D. A. (2004). The KinI kinesin Kif2a is required for bipolar spindle assembly through a functional relationship with MCAK. *J. Cell Biol.* **166**, 473-478.

Garrett, S., Auer, K., Compton, D. A. and Kapoor, T. M. (2002). hTPX2 is required for normal spindle morphology and centrosome integrity during vertebrate cell division. *Curr. Biol.* **12**, 2055-2059.

Gergely, F., Draviam, V. M. and Raff, J. W. (2003). The ch-TOG/XMAP215 protein is essential for spindle pole organization in human somatic cells. *Genes Dev.* **17**, 336-341.

Gorlich, D., Seewald, M. J. and Ribbeck, K. (2003). Characterization of Ran-driven cargo transport and the RanGTPase system by kinetic measurements and computer simulation. *EMBO J.* **22**, 1088-1100.

Gruss, O. J. and Vernos, I. (2004). The mechanism of spindle assembly: functions of Ran and its target TPX2. *J. Cell Biol.* **166**, 949-955.

Gruss, O. J., Wittmann, M., Yokoyama, H. R., Pepperkok, R., Kufer, T., Silljé, H., Karsenti, E., Mattaj, I. W. and Vernos, I. (2002). Chromosome-induced microtubule assembly mediated by TPX2 is required for spindle formation in HeLa cells. *Nat. Cell Biol.* **4**, 871-879.

Guarguaglini, G., Renzi, L., D'Ottavio, F., Di Fiore, B., Casenghi, M., Cundari, E. and Lavia, P. (2000). Regulated Ran-binding protein 1 activity is required for organization and function of the mitotic spindle in mammalian cells in vivo. *Cell Growth Differ.* **11**, 455-465.

Hagting, A., Jackman, M., Simpson, K. and Pines, J. (1999). Translocation of cyclin B1 to the nucleus at prophase requires a phosphorylation-dependent nuclear import signal. *Curr. Biol.* **9**, 680-689.

Hauf, S., Cole, R. W., LaTerra, S., Zimmer, C., Schnapp, G., Walter, R., Heckel, A., van Meel, J., Rieder, C. L. and Peters, J. M. (2003). The small molecule Hesperadin reveals a role for Aurora B in correcting kinetochore-microtubule attachment and in maintaining the spindle assembly checkpoint. *J. Cell Biol.* **161**, 281-294.

Hsu, J. M., Lee, Y. C., Yu, C. T. and Huang, C. Y. (2004). Fbx7 functions in the SCF-complex regulating Cdk1-cyclin B-phosphorylated hepatoma up-regulated protein (HURP) proteolysis by a proline-rich region. *J. Biol. Chem.* **279**, 32592-32602.

Jackman, M., Lindon, C., Nigg, E. A. and Pines, J. (2003). Active cyclin B1-Cdk1 first appears on centrosomes in prophase. *Nat. Cell Biol.* **5**, 143-148.

Joseph, J., Liu, S. T., Jablonski, S. A., Yen, T. J. and Dasso, M. (2004). The RanGAP1-RanBP2 complex is essential for microtubule-kinetochore interactions in vivo. *Curr. Biol*. **14**, 611-617.

Kalab, P., Pu, R.T. and Dasso M. (1999). The Ran GTPase regulates mitotic spindle assembly. *Curr. Biol.* **9**, 481-484.

Kalab, P., Pralle, A., Isacoff, E. Y., Heald, R. and Weis, K. (2006). Analysis of a RanGTP-regulated gradient in mitotic somatic cells. *Nature* **440**, 697-701.

Kehlenbach, R. H., Dickmanns, A., Kehlenbach, A., Guan, T. and Gerace, L. (1999). A role for RanBP1 in the release of CRM1 from the nuclear pore complex in a terminal step of nuclear export. *J. Cell Biol.* **145**, 645-657.

Kéryer, G., Di Fiore, B., Celati, C., Lechtreck, K. F., Mogensen, M., Delouvée, A., Lavia, P., Bornens, M. and Tassin, A. M. (2003). Part of Ran is associated with AKAP450 at the centrosome. Involvement in microtubule organizing activity. *Mol. Biol. Cell* **14**, 4260-4271.

Kline-Smith, S. L., Khodjakov, A., Hergert, P. and Walczak, C. E. (2003). Depletion of centromeric MCAK leads to chromosomecongression and segregation defects due to improper kinetochore attachments. *Mol. Biol. Cell* **3**, 1146-1159.

Knowlton, A. L., Lan, W. and Stukenberg, P. T. (2006). Aurora B is enriched at merotelic attachment sites, where it regulates MCAK. *Curr. Biol.* **16**, 1705-1710.

Koffa, M. D., Casanova, C. M., Santarella, R., Kocher, T., Wilm, M. and Mattaj, I. W. (2006). HURP is part of a Ran-dependent complex involved in spindle formation. *Curr. Biol.* **16**, 743-754.

Kufer, T. A., Silljé, H. H., Korner, R., Gruss, O. J., Meraldi, P. and Nigg, E. A. (2002). Human TPX2 is required for targeting Aurora-A kinase to the spindle. *J. Cell Biol.* **158**, 617-623.

Li, H. Y., Ng, W. P., Wong, C. H., Iglesias, P. A. and Zheng. Y. (2007) Coordination of chromosome alignment and mitotic progression by the chromosome-based Ran signal. *Cell Cycle* **6**, 1886-1895.

Moore, J. D. (2001). The Ran-GTPase and cell-cycle control. *BioEssays* **23**, 77-85.

Musacchio, A. and Salmon, E. D. (2007). The spindle-assembly checkpoint in space and time. *Nat. Rev. Mol. Cell Biol.* **8**, 379-393.

Nevo, R., Brumfeld, V., Elbaum, M., Hinterdorfer, P. and Reich, Z. (2004). Direct discrimination between models of protein activation by single-molecule force measurements. *Biophys. J.* **87**, 2630-2634.

Ookata, K., Hisanaga, S., Bulinski, J. C., Murofushi, H., Aizawa, H., Itoh, T. J.,Hotani, H., Okumura, E., Tachibana, K. and Kishimoto, T. (1995). Cyclin B interaction with microtubule-associated protein 4 (MAP4) targets p34cdc2 kinase to microtubules and is a potential regulator of M-phase microtubule dynamics. *J. Cell Biol.* **128**, 849-862.

Plafker, K. and Macara, I. G. (2002). Fluorescence resonance energy transfer biosensors that detect Ran conformational changes and a Ran x GDP-importin-b-RanBP1 complex in vitro and in intact cells. *J. Biol. Chem.* **277**, 30121-30127.

Richards, S. A., Lounsbury, K. M. and Macara, I. G. (1995). The C-terminus of the nuclear RAN/TC4 GTPase stabilizes the GDP-bound state and mediates interactions with RCC1, RAN-GAP, and HTF9A/RANBP1. *J. Biol. Chem.* **270**, 14405-14411.

Salina, D., Enarson, P., Rattner, J. B. and Burke, B. (2003). Nup358 integrates nuclear envelope breakdown with kinetochore assembly. *J. Cell Biol.* **162**, 991-1001.

Santarella, R. A., Koffa, M. D., Tittmann, P., Gross, H. and Hoenger, A. (2007). HURP wraps microtubule ends with an additional tubulin sheet that has a novel conformation of tubulin. *J. Mol. Biol*. **365**, 1587-1595.

Silljé, H. H., Nagel, S., Korner, R. and Nigg, E. A. (2006). HURP is a Ran-importin b-regulated protein that stabilizes kinetochore microtubules in the vicinity of chromosomes. *Curr. Biol.* **16**, 731-742.

Smith, A. E., Slepchenko, B. M., Schaff, J. C., Loew, L. M. and Macara, I. G. (2002). Systems analysis of Ran transport. *Science* **295**, 488-491.

Trieselmann, N. and Wilde, A. (2002). Ran localizes around the microtubule spindle in vivo during mitosis in Drosophila embryos. *Curr. Biol.* **12**, 1124-1129.

Tsai, M. Y., Wiese, C., Cao, K., Martin, O., Donovan, P., Ruderman, J., Prigent, C. and Zheng, Y. (2003). A Ran signalling pathway mediated by the mitotic kinase Aurora A in spindle assembly. *Nat. Cell Biol.* **5**, 242-248.

Verde, F., Dogterom, M., Stelzer, E., Karsenti, E. and Leibler, S. (1992). Control of microtubule dynamics and length by cyclin A- and cyclin B-dependent kinases in Xenopus egg extracts. *J. Cell Biol.* **118**, 1097-1108.

Weis, K. (2003). Regulating access to the genome: nucleocytoplasmic transport throughout the cell cycle. *Cell* **112**, 441-451.

Wong, J. and Fang, G. (2006). HURP controls spindle dynamics to promote proper interkinetochore tension and efficient kinetochore capture. *J. Cell Biol.* **173**, 879-891.

Journal of Cell Science